Monitoring ENSO in COADS with a Seasonally Adjusted Principal Component Index

Klaus Wolter and Michael S. Timlin
Cooperative Institute for Research in Environmental Sciences, University of Colorado
Boulder, CO 80309-0449

MOTIVATION

This paper summarizes an ongoing effort to create a multivariate ENSO index that is based on long-term marine records from the Comprehensive Ocean-Atmosphere Data Set (COADS; Woodruff et al., 1987). Instead of monitoring a single ocean-atmosphere variable such as SST or SLP, this index presents a weighted average of the full multivariate signal of ENSO. Walker and Bliss (1932) already examined precipitation, temperature and pressure fields in conjunction, so this is not a new approach. We also want to allow for seasonal variations in the evolution of ENSO, because most anomaly fields show considerable variation with the annual cycle (see Fig. 2 below). Therefore, our index is computed such that each seasonal index value is standardized with respect to its season's observed variability.

APPROACH

Balancing the need for a long record with data quality considerations, we chose the last four decades (1950-90) of the trimmed COADS record in the tropical Pacific domain (Fig. 1). Outliers in monthly 4°x4° means were removed if they deviated by more than 4.5 standard deviations from the 1950-90 base period monthly mean. Missing values were interpolated up to 4 months, while longer gaps were filled with long-term mean values. Monthly means were averaged into bimonthly seasons (DJ, JF, ..., ND) to filter out 30-60 day oscillations. Subsequently, a spatial cluster analysis (Wolter, 1987) was performed in order to focus on large-scale features of tropical Pacific variability. Spatial clusters maximize the internal correlation within each cluster, hence cluster time series are more robust than other, more arbitrary area averages. Assuming stationarity, clusters are especially useful when going back in time to lower observational densities, an issue not further pursued in this paper.

The main step in this analysis sequence is a combined principal component analysis (PCA) of all analyzed cluster fields, namely, sea level pressure (P), zonal and meridional wind component (U,V), sea surface and air temperature (S, A), and total cloudiness (C). All twelve seasons were analyzed separately to document the behavior of the ENSO phenomenon, which emerges as the first unrotated PC in every season. With regard to the PCA input, one can choose either anomaly or standardized time series for each cluster. This corresponds to either using covariance or correlation matrix based PCA. In the former case, each anomaly cluster time series is multiplied with the square root of its area to preserve the variance of the full field. Given the strong circulation anomalies of ENSO, either approach yields similar loading patterns and PC time series, but the covariance-based case is easier to update. A final issue is how to combine different variables in covariance-based PCA. Lorenz (1956) already discussed this problem without actually performing such an analysis. We set the field variance of each of six fields to the same level, while preserving the local variance changes within the field. Inflating the variance of the primary fields (P, S) compared to the rest (U,V,A,C) made little difference in loading patterns, explained variance, and time series of the first PC, so we kept the simplest solution, equal total variance for each field.

ASPECTS OF THE SEASONAL CYCLE OF ENSO

Among the twelve seasonal loading maps of ENSO, only the patterns for December/ January (DJ) are shown here (Fig. 1), this being the peak season in terms of explained variance. However, a sense of the seasonal cycle of ENSO can be extracted from the migrations of the 'centers of action' (see Fig. 2 below). The loading patterns depicted in Fig. 1 are standardized to represent the local correlation of each cluster with the first covariance-based PC of DJ 1950-90. Lightly dotted squares in Fig. 1 are not clustered. Positive loadings translate into positive anomalies during an ENSO event. In the following, all six fields are discussed from top (P) to bottom (C):

P: We recognize the classic dipole structure of the Southern Oscillation, however, with the western dipole centered north of the equator, and the eastern dipole stretching roughly from Tahiti to Central America. Many high loadings at either end of the pressure seesaw lie north or on the equator, attesting to the global character of this phenomenon.

U: Strong positive loadings in the central equatorial Pacific are surrounded by negative loadings, most notably over the maritime continent and the eastern Pacific. Given the average flow field of tradewind easterlies, anomalous convergence/divergence is implied at the eastern/western edge of the positive loading center during ENSO events.

V: Strong negative loadings (anomalous northerlies) lie on top and to the north of the average position of the ITCZ, positive loadings (anomalous southerlies) well to the south. This corresponds to the well-known southward shift of the ITCZ during ENSO events (Rasmussen and Carpenter, 1982). U and V anomalies in combination denote anomalous convergence from the dateline to about 120°W, along and south of the equator. Weakened northerlies (positive loadings) over the South China Sea go along with weaker easterlies (positive loadings) north of 14°N.

S: This panel features the largest explained variance(52%), anchored by several loadings in the central and eastern Pacific that represent more than 75% local variance. We recognize the signature of the mature ENSO event phase (Rasmussen and Carpenter, 1982): strong positive SST anomalies in the eastern Pacific, flanked by negative anomalies in the subtropics near the dateline, and positive anomalies again in the western Pacific, which is mainly a northern winter feature.

A: Air temperature loadings mirror SST loadings, but are weaker negative in the subtropics, and stronger positive in the western Pacific, suggesting that global tropical warming is communicated better through the atmosphere than the ocean during ENSO events.

C: This loading map shows a clear increase in cloudiness over the central south equatorial Pacific during ENSO, just about where to expect it from the convergence patterns implied in U and V. The simultaneous decrease in cloudiness over the northwest tropical Pacific matches the wind patterns described above, as well as the regional increase in temperature.

Turning our attention to Fig. 2, we see the seasonal migration of the main 'centers of action' in each of four commonly monitored fields (P,U,S,C). Centers of action were determined by decreasing a positive or negative loading threshold until at least twenty 4°x4° squares exceeded it, after which their weighted average determined their geographic center of gravity. Comparisons can be made with conventional, geographically fixed indices for each variable (based on Table T1 in recent issues of the 'Climate Diagnostics Bulletin').

P: The eastern dipole is in its northernmost position in DJ, gets closest to Tahiti in FM, and then moves back to its easternmost position in AM, thereafter staying north of 10°S. The western dipole starts near the equator during northern winter, reaches its northeasternmost position in MA (>10°N), then circles back to its southern extreme (near Darwin) in JJ, finally drifting slowly northward. Total movement of both centers of action is considerable (>1000km), which two stations alone (such as Tahiti and Darwin) cannot adequately represent.

U: The center of westerly anomalies during an ENSO event moves eastward from its extreme western position in JJ to its extreme eastern position in DJ, while its seasonal march back is less regular. It matches the western conventional 850 mb box wind box from JJ through SO, while the rest of the year the central and western box are straddled, and the eastern

box remains irrelevant throughout. However, the westernmost box is affected by opposite anomalies in the western Pacific which encroach upon it during ND and MA, raising the danger of mixed signals during northern winter.

S: The main ENSO SST loading center stays within ENSO region 3, however, during northern spring (MAM) it sags slightly to the south of it. ENSO 12 is irrelevant for monitoring ENSO as a basin-wide phenomenon. ENSO 4 gets some of its signal from the negative loadings of the SPCZ, raising again the danger of mixed signals.

C: This field has the strongest annual cycle of loading strength for its primary center of action. The OLR-based monitoring box coincides reasonably well with the cloudiness center of action, except for FMAM when the main cloudiness anomaly migrates into the eastern Pacific. Negative loadings (drought) over the maritime continent are present all year round, mainly north of the equator. In northern summer and fall, this signal is stronger than the increase in central Pacific cloudiness, denoting the monsoonal link to ENSO.

In sum, the ENSO 3 SST box is the best conventional univariate ENSO index, OLR and U boxes are more or less representative of their respective fields most of the year, while Tahiti and Darwin never hit either pressure dipole at the same time of the year.

RECENT ENSO EVENTS

Figure 3a shows the ENSO PC time series for the well-known ENSO events 1957/58, 65/66, and 72/73, the three main events in Rasmussen and Carpenter's (1982) composites. The timeseries is standardized for each season, it shows the common rapid onset and early peak in AM through JA, with a steady high amplitude through the rest of the year, and a secondary maximum in DJF. The subsequent decline is irregular, and may lead to a quick cold event (73/74) or a delayed one (67), or even a second warm event (59). Figure 3b documents the ENSO PC timeseries for the last three events: 1982/83, 86/87, and 91/92 (preliminary data). After the rapid onset in northern spring/early summer, all three recent events grew through the second half of the year until the next spring (FMAM), at a time when the previous three events were already decaying (Fig. 3a). Starting with an eastward propagation of SST anomalies from the central Pacific rather than from the American coast westward, the most recent events peaked later than previous events and have ended later as well. Possibly not unrelated, the last three events all resulted in peak anomalies larger than the previous ones.

Acknowledgments

This research has been supported through NOAA's EPOCS and Climate and Global Change Programs.

REFERENCES

Lorenz, E. N., 1956: Empirical Orthogonal Functions and Statistical Weather Prediction. M.I.T. Dept. of Meteorology, Sci. Rpt. No. 1, Contract AF19 (604)-1566, 49pp.

Rasmusson, E. G., and T. H. Carpenter, 1982: Variations in tropical sea surface temperature and surface wind fields associated with the Southern Oscillation/El Nîno. *Mon. Wea. Rev.*, **110**, 354 - 384.

Walker, G. T., and E. W. Bliss, 1932: World weather V. *Mem. Roy. Meteorol. Soc.*, **4**, 53 - 84.

Wolter, K., 1987: The Southern Oscillation in surface circulation and climate over the tropical Atlantic, Eastern Pacific, and Indian oceans, as captured by cluster analysis. *J. Climate Appl. Meteor.*, **26**, 540 - 558.

Woodruff, S. D., Slutz, R. J., Jenne, R. L., and P. M. Steurer, 1987: A comprehensive ocean-atmosphere data set. *Bull. Amer. Meteor. Soc.*, **68**, 1239 - 1250.

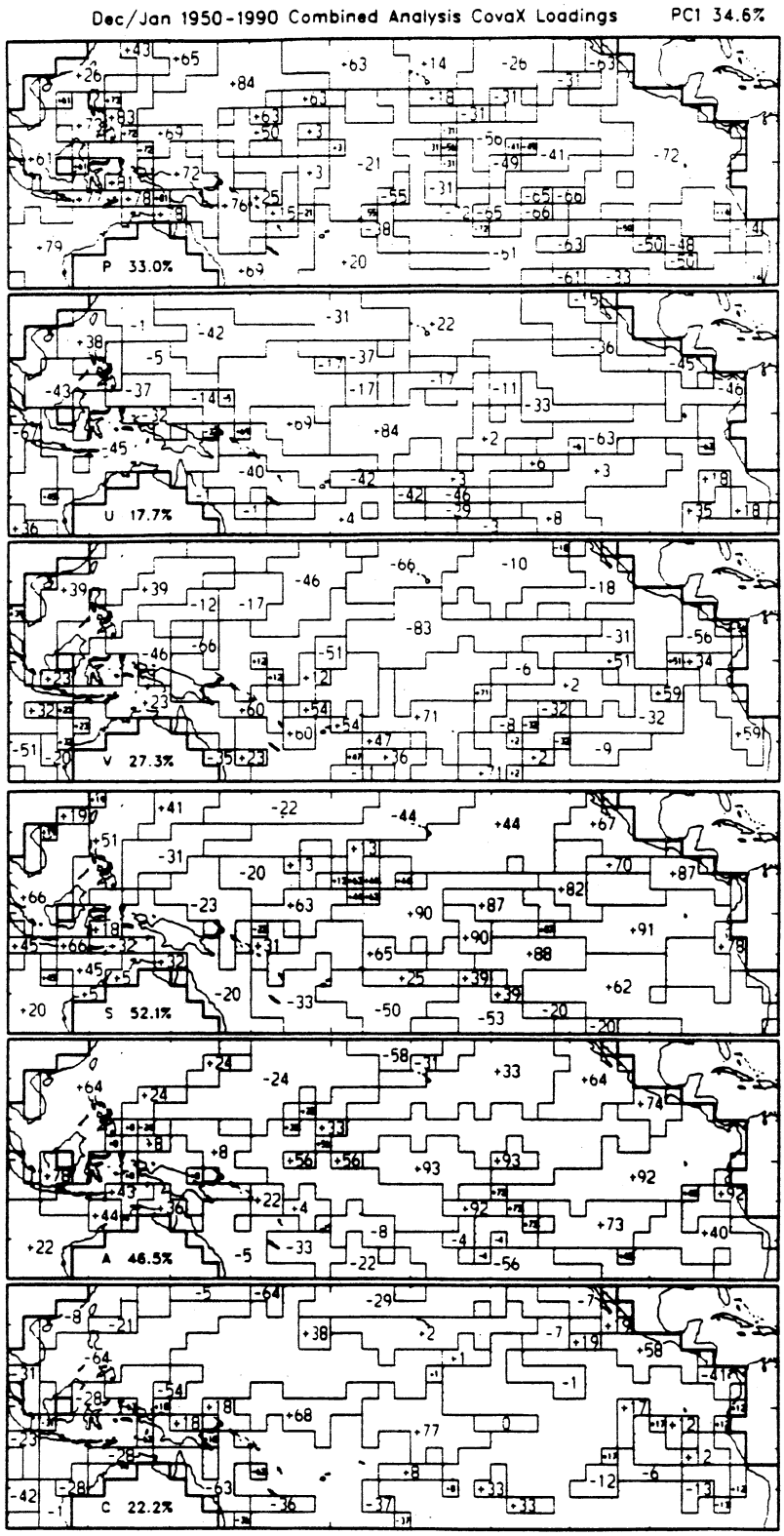

Fig. 1. Loading maps of the first combined unrotated principal component in tropical Pacific cluster fields for December/January during 1950-90. Total explained variance is given at the top, while individual field variances are listed next to the variable indicator in the bottom left corner of each panel (P = SLP; U,V = zonal and meridional wind components; S,A = sea surface and air temperature; C = total cloudiness). Loadings are given in hundredths. Lightly dotted regions are not clustered.

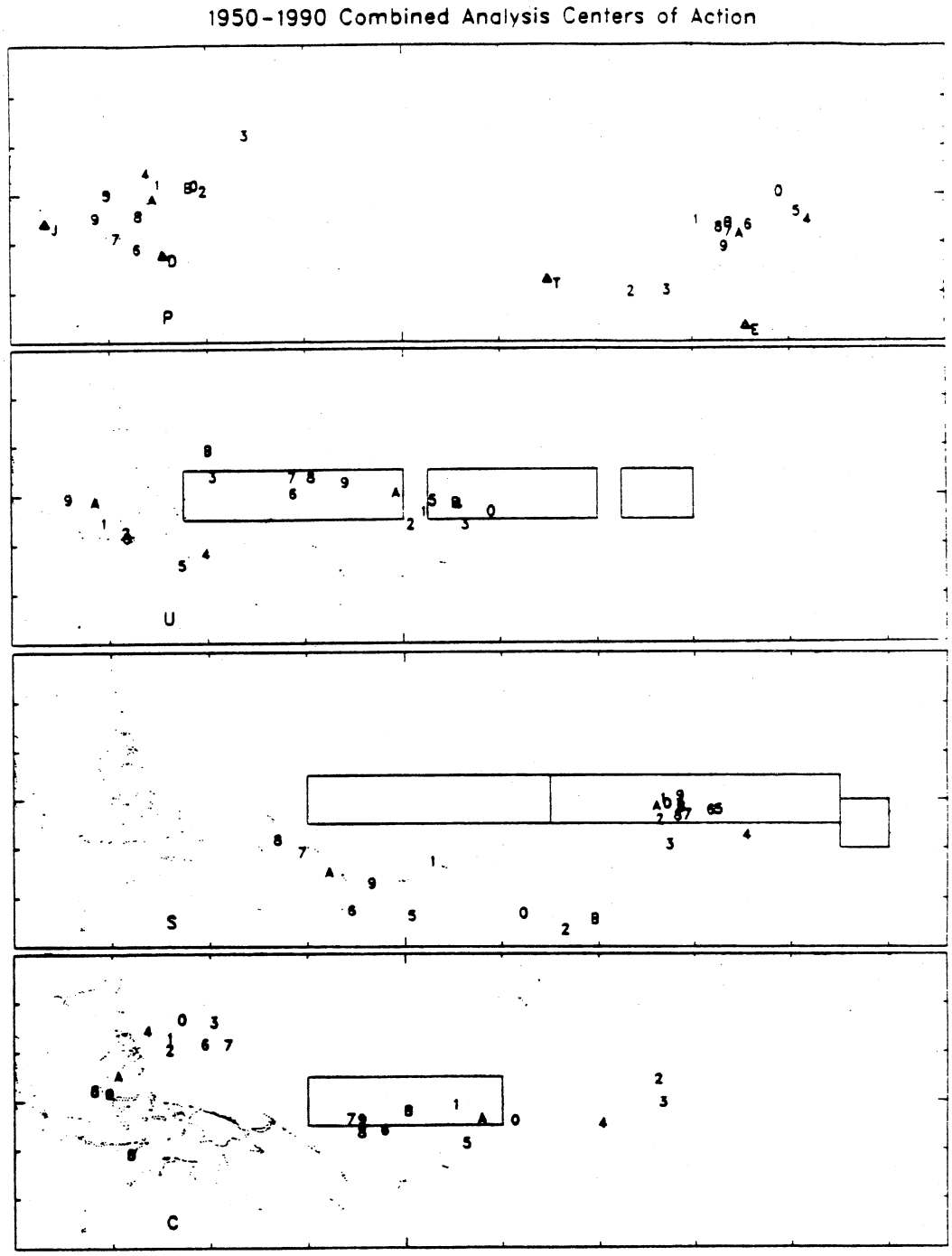

Fig. 2. 'Centers of action' of the first combined unrotated principal component in tropical Pacific cluster fields for all twelve bimonthly seasons (0 = DJ, 1 = JF, ..., 9 = SO, A = ON, and B = ND) during 1950-90. Panels for P, U, S, and C are shown. Sea level pressure stations are denoted by triangles and J for Jakarta, D for Darwin, T for Tahiti, and E for Easter Island. Regularly published 850 mbar zonal wind , SST, and OLR index boundaries are taken from Table T1 in recent 'Climate Diagnostics Bulletin' issues.

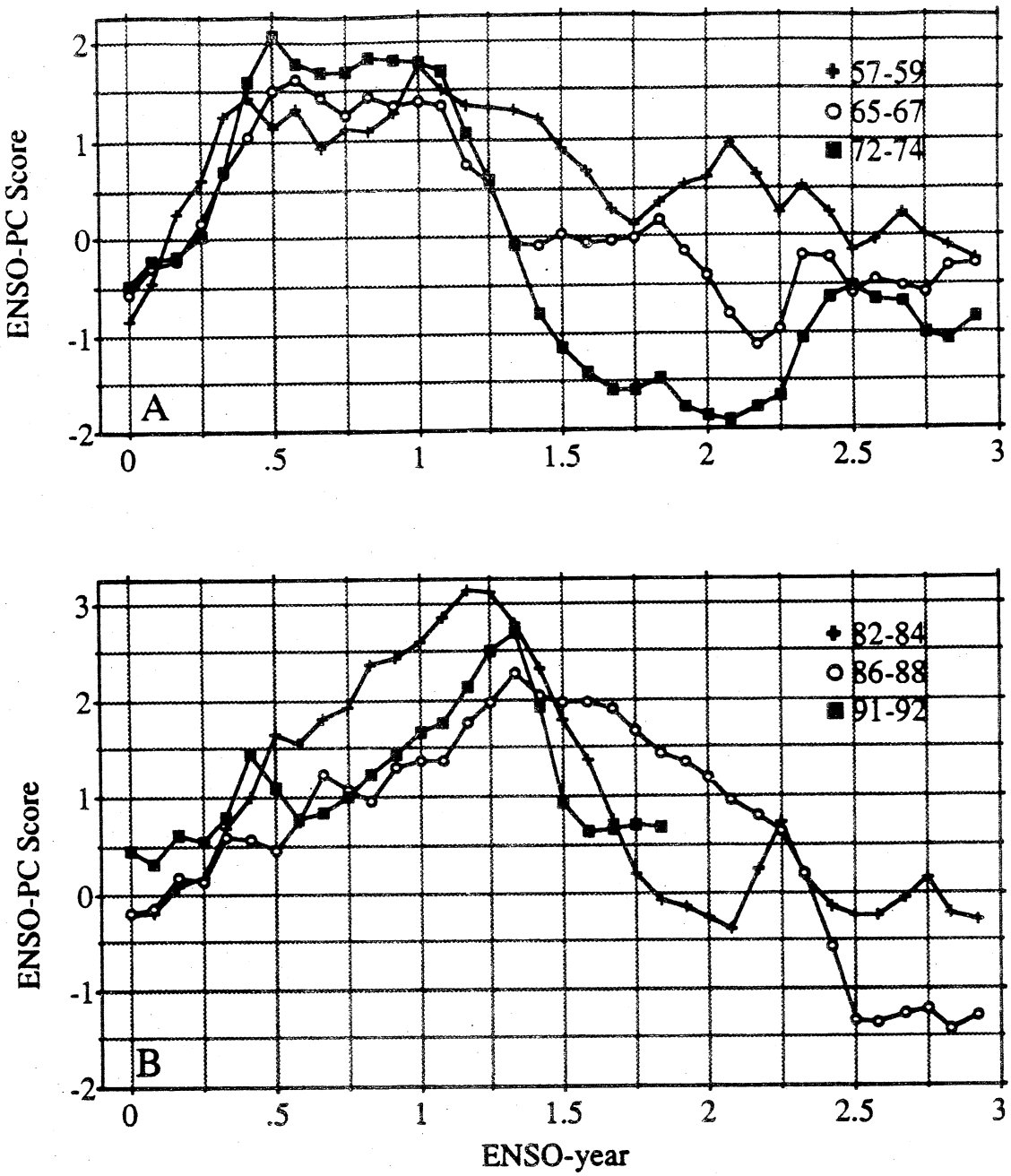

Fig. 3. Time series ('ENSO-PC score') of the first combined unrotated principal component in tropical Pacific cluster fields, analyzed separately for each of twelve sliding bimonthly seasons. Panel A shows time series for the three ENSO events 1957/58, 65/66, and 72/73, and panel B for 1982/83, 86/87, and 91/92. A score of one represents a full standard deviation departure of this PC for the respective season involved, defined positively for ENSO events. Each time series starts with December/January of the onset year (e.g., December 56/January 57).